Prediction of DSRC Service Over-reach inside an Arched Transportation Tunnel

Gilbert Siy Ching[*1], Mir Ghoraishi[*2], Navarat Lertsirisopon[*1], Jun-ichi Takada[*1], Itoji Sameda[*3], Ryuji Soma[*4], Hironori Sakamoto[*5], and Tetsuro Imai[*6]

*Department of International Development Engineering[*1], (The Center for Research and Development of Educational Technology) [*2], Tokyo Institute of Technology (2-12-1-S6-4, O-okayama, Meguro-ku, Tokyo, Japan, 152-8552, +81-3-5734-3288, gilbert@ap.ide.titech.ac.jp,mir@nh.cradle.titech.ac.jp,{joy, takada}@ap.ide.titech.ac.jp)*

*Japan Highway Public Corporation[*3] (currently with West Nippon Expressway Co. Ltd., Japan), (1-6-20 Dojima, Kita-ku, Osaka, Japan, 530-0003, i.sameda.aa@w-nexco.co.jp)*

*Central Nippon Expressway Co. Ltd., Japan[*4], (1305-3 Naganuma-machi, Hachioji-shi, Tokyo, Japan, 192-0907, r.soma.aa@c-nexco.co.jp)*

*Highway Telecom Engineering Co., Ltd., Japan[*5], (h-sakamoto@dtenet.co.jp)*

*Radio Access Network Development Department, NTT DoCoMo Inc., Japan [*6], (3-5 Hikari-no-oka, Yokosuka-shi, Kanagawa, Japan 239-8536, imait@nttdocomo.co.jp*

Inside tunnels, the possibility of over-reach of radiated power from the Dedicated Short Range Communications (DSRC) service zone to the out-of-service zone is high, since the waves are confined in the tunnel space. To inspect this more carefully, wideband directional channel measurements were conducted inside an arched transportation tunnel, and the gain, angle-of-arrival and delay of each propagation path were estimated from the measured data. These propagation paths reveal that paths scattered from ground and sidewalk are the dominant factors that cause the over-reach of radiated power. This then suggests that the ground and sidewalk paths together with the LoS path can be used to predict the over-reach inside a typical transportation tunnel.

***Keywords**: DSRC, over-reach, tunnel propagation, wideband directional measurements*

1. Introduction

As communities progress, roads and highways are built to connect between communities. For any highway network, tunnels form an integral part of the infrastructure since it reduces travel time as compared to going around an obstacle. However, as mobility increases, vehicular accidents also increase. Therefore there is a growing interest in intervehicular and vehicle-roadside communications in improving driver safety, security and comfort [1]-[3]. Moreover, in emergency situations, people can be trapped inside tunnels as compared to open roads.

A popular service of vehicle-roadside communications is the electronic toll collection [4], which is an application of the Dedicated Short Range Communications (DSRC) system. DSRC is a short to medium range communication service intended to improve public safety on the road and also to exchange high speed duplex data between roadside units (RSU) and onboard units (OBU) installed inside vehicles [5]. Future DSRC services envisioned include traffic advisory, collision avoidance and location awareness service among others. To deploy such services, it is required to limit the radiated power in the service zone to prevent undesired communication by over-reach of the radiated power to the out-of-service zone or simply out-of-zone. Inside transportation tunnels, the implementation of such application becomes an even more demanding task. This is because the propagation of radio waves inside tunnels are confined in the tunnel space which can increase the received power in the out-of-zone.

To inspect this over-reach effect, a detailed knowledge of the radio channel inside tunnel is necessary. Although a wide range of research [6]-[10] addressing the communication channel inside tunnels, both theoretically and experimentally, are available, the scenarios in which these analyses have been conducted do not match the DSRC system. Sample applications of the past researches conducted inside tunnels were for distributed antenna sys-

tems [11], multiple-input-multiple-output (MIMO) systems [12] and future cellular applications [13]. For the inspection of the over-reach in the DSRC service out-of-zone however, it is essential to analyze the propagation channel for this particular scenario.

Focusing on the over-reach analysis of the DSRC system, we conducted a channel sounding campaign inside an arched tunnel for 2 transmitter (Tx) positions and 204 receiver (Rx) points covering all traffic lanes in the DSRC out-of-zone. A cylindrical antenna array was utilized with 96 dual polarized elements at the Rx to measure the full 360° azimuthal direction. A multidimensional maximum likelihood algorithm was then used to estimate the parameters of the received propagation paths. This method was chosen instead of ray tracing methods or computational electromagnetic tools like FDTD (finite-difference time-domain) because ray tracing methods cannot handle curve surfaces, while it is not practical to use FDTD to solve scenarios whose size is thousand times larger than the wavelength. In our previous work [14] - [15], the mean received power on the out-of-zone was obtained and the significant scatterers were identified. In this study, aside from the delay spread, the probability of over-reach caused by the fading of the received power is simulated and observations to predict over-reach is given.

The paper is organized as follows. The DSRC standard in Japan is discussed in section 2 followed by the details of the measurement campaign in section 3. The parameter estimation process is also described including the identification of single-bounce or multiscattering paths and classification of the dominant scatterers based on the tunnel structure. The computation of delay spread and cumulative distribution function of received power due to fading is presented in section 4, followed by the discussion of the over-reach prediction in section 5 before giving the conclusions in section 6. Note that the term 'scattering' is used throughout this paper to express any kind of interaction between propagating wave and the structure of the tunnel unless otherwise mentioned.

2. DSRC standard in Japan

The DSRC system standard in Japan is covered in the Association of Radio Industries and Businesses' (ARIB) STD-T75 [16] and STD-T88 [17]. It specifies the radio communication interface between a RSU and an OBU installed on a land vehicle operating in the 5.8 GHz band. Since 2001, the DSRC system has been put into use in the form of the ETC system. Other intended services include road and traffic information as well as location awareness systems. For these purposes, the communication area is limited and within 30 m from the RSU (assumed Tx in this study), the received power at the OBU (assumed Rx in this study) should be from -56 to -40 dBm. Outside the communication zone, the received power should be less than -70.5 dBm to avoid undesired communications. Some technical specifications are shown in Table 1 and an example of a DSRC communication coverage zone is shown in Fig. 1(a).

Table 1 DSRC technical specifications

Parameter	Limits
OBU Rx antenna gain	$<$ 10 dBi
OBU Rx received power	Inside DSRC zone: -56 to -40 dBm Outside DSRC zone: < -70.5 dBm
RSU Tx transmit power	$<$ 24.8 dBm (300 mW)
RSU Tx antenna gain	$<$ 20 dBi
RSU and OBU polarization	right hand circular
DSRC system bandwidth	4.4 MHz

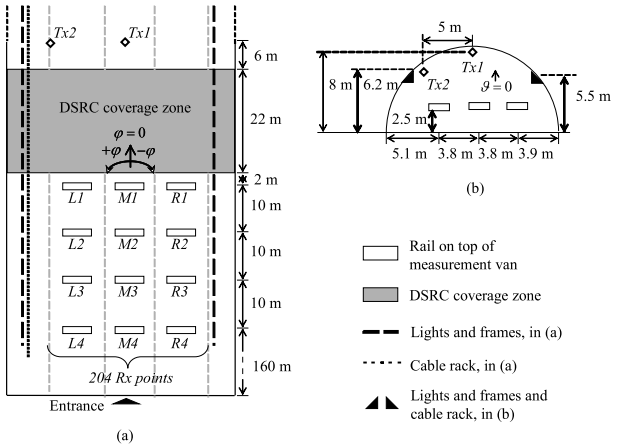

Figure 1 (a) Measurement scenario. (b) Front view from tunnel entrance.

3. Channel sounding

A measurement campaign aiming at the over-reach analysis of the DSRC system was managed in a highway tunnel in the second Tomei highway, Shizuoka prefecture, Japan. In the following subsections we will describe the measurement scenario, channel sounder, algorithm for extracting the propagation paths and procedure for path classification according to the tunnel structure.

3.1. Scenario and equipment

The measurements were conducted in a transportation tunnel with a semicircular arched cross section. The arched tunnel used is a typical tunnel since nowadays, a

Table 2 Measurement parameters

Description	Value
Center frequency, f_c	5.2 GHz
Bandwidth	100 MHz
Delay resolution	10 ns
Maximum delay	6.4 μs
Tx signal	multitone
Tx power	40 dBm
Tx antenna	vertically aligned sleeve dipole
Tx antenna height	8 m (Tx1), 6.2 m (Tx2)
Rx antenna array	cylindrical, 4 rings $\times$ 24 dual polarized patch elements
Rx antenna height	2.5 m
Rx points	204 points for both Tx1 and Tx2
Synchronization	Cesium clocks
Noise floor	< -85 dBm

lot of tunnels are dug using tunnel boring machines [18] and the lower half is leveled to form an arched tunnel. The tunnel can accommodate up to 3 car lanes and is 16.6 m wide on the ground level. The maximum height at the center of the cross section is 8.5 m. At the measurement time, the tunnel was under construction but some structures were already installed as shown in Fig. 1(a). For the scatterer identification in next sections, we classify the tunnel structure as follows:

- *ground*; the floor of the tunnel that includes the 3 car lanes but excludes the sidewalks.
- *left and right sidewalks*; located at the sides of the ground of the tunnel.
- *left and right light-frames*; the framing for the lights and cable racks.
- *left and right walls*; defined as the portion between light-frames and the ground.
- *ceiling*; defined as the portion above the light-frames.

For the measurement equipment, the RUSK-DoCoMo channel sounder [19] was employed with the related parameters found in Table 2. A wideband multitone signal of 100 MHz bandwidth centered at 5.2 GHz sounds the tunnel propagation channel. The center frequency of 5.2 GHz was used instead of 5.8 GHz due to the limitation of the channel sounder. A vertical sleeve dipole was used at the Tx whereas the Rx antenna array was composed of 96 dual-polarized patches from 4 rings of 24 dual-polarized elements each, to be able to measure the full 360° azimuthal direction.

To eliminate the frequency response of the cables and system, the calibration function incorporated in the sounder was utilized before making the measurements.

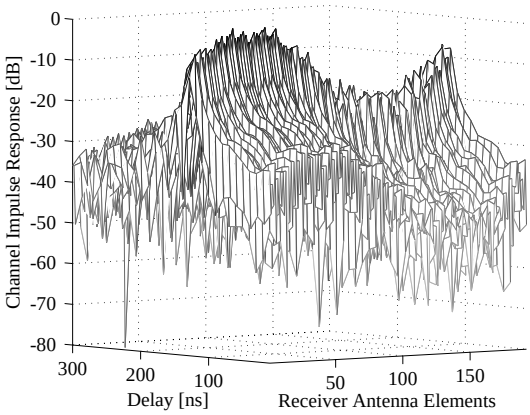

Figure 2 Sample channel impulse response for each receiver antenna elements at Tx1, M1-Rx17.

During the measurements, the channel impulse response was taken from each element using a fast RF switch and stored in a hard disk for off-line processing. Cesium clocks at both Tx and Rx are available for synchronization. With the employed Rx antenna array, both vertically and horizontally polarized received waves could be analyzed. As the Tx antenna is always vertically polarized, vertical and horizontal polarizations at the Rx are called copolarization and cross-polarization throughout the paper.

Since we want to identify the propagation mechanism that may cause interference in the out-of-zone, the measurement campaign was performed in 2 rounds outside of the DSRC coverage zone as depicted in Fig. 1. For the Rx antenna array, it was mounted on a rail on top of the measurement van for a height of 2.5 m from the ground with line-of-sight (LoS) to the Tx antenna. The measurement van moved to 12 different locations to cover the out-of-zone. The van locations are denoted as L1 to L4, M1 to M4 and R1 to R4, corresponding to the left, middle and right lanes respectively. In each van location, the Rx antenna array moved along the rail in 17 different points denoted as Rx1 to Rx17 from left to right for each van location, bringing the total number of Rx points to 204 for each Tx case. A sample measurement data for Tx1, M1-Rx17 is shown in Fig. 2 which represents the channel impulse response of the 192 receiver antenna elements.

3.2. Path extraction and classification

To extract the propagation paths from the measurement data like the one shown in Fig. 2, a multidimensional maximum likelihood algorithm was used. The signal model of the algorithm is composed of discrete paths and dense multipath components. For the discrete paths, the channel model equation for the static and single-input-

Table 3 Estimated Path Parameters for Tx1, M1-Rx17. 'l' means left whereas 'r' means right.

path index	g [dB]	$c\tau$ [m]	φ [deg]	ϑ [deg]	g_{C} [dB]	g_{X} [dB]	scatterer (bounce type)
1	-80	31	5	80	-80	-94	LoS path
	(-75)	(31)	(3)	(80)	(-75)		
2	-94	35	-26	103	-96	-98	r-sidewalk (single-bounce)
3	-97	34	23	80	-100	-101	l-light-frame (single-bounce)
4	-98	32	5	109	-99	-103	ground
	(-102)	(32)	(3)	(109)	(-102)		(single-bounce)
5	-99	33	-15	76	-100	-105	r-light-frame (single-bounce)

multiple-output (SIMO) propagation channel is:

$$\mathbf{h}(s,\tau,\varphi,\vartheta) = \sum_{l=1}^{L(s)} \begin{bmatrix} \gamma_{\mathrm{C},l} \\ \gamma_{\mathrm{X},l} \end{bmatrix} \times\delta(\tau-\tau_l)\delta(\varphi-\varphi_l)\delta(\vartheta-\vartheta_l) \quad (1)$$

where s refers to the position of the receiver, $L(s)$ is the number of propagation paths in that position, $\gamma_{\mathrm{C},l}$ and $\gamma_{\mathrm{X},l}$ are the complex copolarization and cross-polarization path weights respectively, τ_l is the delay, φ_l is the azimuth and ϑ_l is the coelevation of the angle-of-arrival (AoA) for path l. $\delta(\cdot)$ is the Dirac delta function. The dense multipath components on the other hand are modeled as the rise of the floor (modeled by an exponential function) above the noise in the delay domain and uniform in the angular domain [20].

The path parameters (path weights, delay and AoA) of the discrete paths are also estimated during the extraction of the discrete paths and dense multipath components. The extracted discrete propagation paths constitute 88% of the received power whereas the remaining 12% of the received power are considered as dense multipath components.

The extracted paths are classified according to the tunnel structure introduced previously. By tracing the AoA from the Rx towards the tunnel, the last scattering point of each extracted path can be identified. This scattering point is then used to classify the extracted path. In addition to the AoA, the delay helps to confirm if the extracted path is a single-bounce scattering (i.e. Tx to tunnel structure to Rx) or multiscattering. Table 3 shows the extracted paths and their estimated parameters for Tx1, M1-Rx17 where the delay τ is expressed as the corresponding path length $c\tau$ in meters, where c is the speed of light. g_l is the path gain defined as

$$g_l = |\,\gamma_{\mathrm{C},l}\,|^2 + |\,\gamma_{\mathrm{X},l}\,|^2 = g_{\mathrm{C},l} + g_{\mathrm{X},l} \quad (2)$$

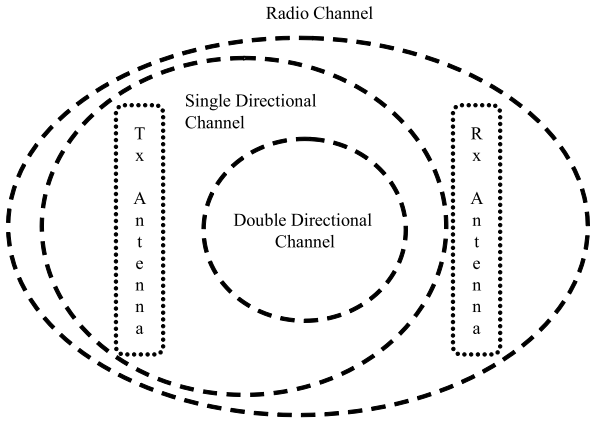

Figure 3 Illustration of double directional channel concept.

The values in parenthesis in Table 3 represent the theoretical values for LoS and ground specular reflection.

4. Over-reach analysis of DSRC service zone

Fig. 3 shows the double directional channel concept [21]. The advantage of the double directional analysis of the channel is that the complex antenna response of the measurement antennas can be deconvolved from propagation paths if the AoAs and angle of departures (AoDs) are known [22]. Although in this analysis, only the AoAs are estimated (i.e. single directional channel), the AoDs φ^{Tx} and ϑ^{Tx} can also be indirectly calculated for LoS and single-bounce paths which comprise 62 % and 35 % respectively of the power of the extracted paths for Tx1, and 70 % and 27 % for Tx2. In the following section, the path parameters together with simulated application antennas will be used to predict the delay spread. Furthermore, the fading of the received power to analyze if over-reach occurs will be examined.

4.1. Application antennas

In the same way that measurement antennas can be deconvolved from the propagation paths, application antennas can be convolved to the propagation paths to predict system parameters like delay spread and received power. Following the limits of the DSRC standard as shown in Table 1, a rectangular patch antenna tilted by $\vartheta = 45^\circ$ along $\varphi = 0^\circ$ is considered for the Rx application antenna and has a maximum gain of 6.4 dBi. For the Tx application antenna, a uniform received power of -48 dBm is assumed in the DSRC zone shown in Fig. 1. The maximum gain of the assumed Tx application antenna will be 18 dBi for the Tx1 case and 19 dBi for the Tx2 case, with a transmitted power P_{t} of 7 dBm. Beyond the DSRC zone,

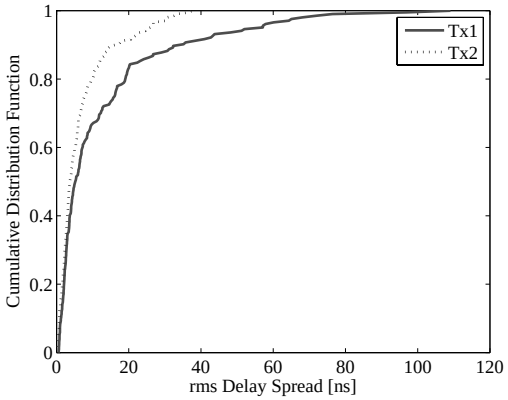

Figure 4 CDF of rms delay spread.

the gain of the assumed Tx application antennas are set to 25 dB below the maximum gain to limit the received power of LoS in the out-of-zone to less than -70.5 dBm.

4.2. Delay spread

To calculate the root-mean-square (rms) delay spread at each position, the radio channel gain of each path is first defined:

$$g_{\mathrm{ch},l}=|\gamma_{\mathrm{ch},l}|^2=\left|\frac{b^{\mathrm{Tx}}(\varphi_l^{\mathrm{Tx}},\vartheta_l^{\mathrm{Tx}})\ \ \gamma_{\mathrm{C},l}\ \ b^{\mathrm{Rx}}(\varphi_l,\vartheta_l)}{b^{\mathrm{D}}(\varphi_l^{\mathrm{Tx}},\vartheta_l^{\mathrm{Tx}})}\right|^2 \quad (3)$$

where b^{Tx}, b^{Rx} and b^{D} are the antenna response of the Rx and Tx application antennas and sleeve dipole respectively. In practice, circularly polarized antennas are used in DSRC systems, but in the measurements, we could use only a vertical sleeve dipole in the Tx side due to the limitation of the instruments. Therefore, only the copolarized components are used in computing $g_{\mathrm{ch},l}$. The rms delay spread for LoS and single-bounce paths L' is then computed as follows:

$$\tau_{\mathrm{rms}}(s)=\sqrt{\frac{\sum_{l=1}^{L'(s)}(\tau_l-\tau_{\mathrm{m}}(s))^2 g_{\mathrm{ch},l}}{\sum_{l=1}^{L'(s)} g_{\mathrm{ch},l}}} \quad (4)$$

where

$$\tau_{\mathrm{m}}(s) \ = \ \frac{\sum_{l=1}^{L'(s)}\tau_l g_{\mathrm{ch},l}}{\sum_{l=1}^{L'(s)} g_{\mathrm{ch},l}} \quad (5)$$

Fig. 4 shows the cumulative distribution function (CDF) of the rms delay spread. Since the delay spread is much smaller than the inverse of the DSRC system bandwidth listed in Table 1, the DSRC system will not be able to distinguish mutipaths in the delay domain and therefore fluctuations in the received power due to the combinations of the multipaths will occur.

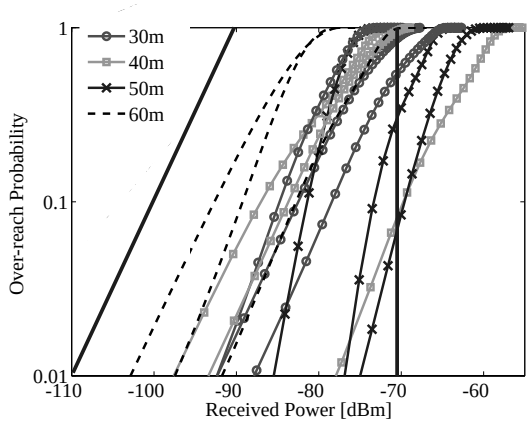

Figure 5 Received power CDF (over-reach probability) for Tx1. Solid line indicates the -70.5 threshold (straight) and theoretical Rayleigh CDF (slanted).

4.3. Fading of received power

To predict the fading of the received power in the out-of-zone, the fading of the total field strength γ_{T} is computed first by assuming the propagation paths have random phase. The CDF of the total field strength can then be derived by the characteristic function method [23]:

$$\mathrm{F}(\mid\gamma_{\mathrm{T}}\mid)=\frac{2\mid\gamma_{\mathrm{T}}\mid}{R}\sum_{n=1}^{\infty}\frac{\Phi(\rho_n/R)}{\rho_n J_1^2(\rho_n)}J_1\left(\frac{\rho_n\mid\gamma_{\mathrm{T}}\mid}{R}\right) \quad (6)$$

$$R \ = \ \sum_{l=1}^{L'(s)}\mid\gamma_{\mathrm{ch},l}\mid+5\sigma \quad (7)$$

$$\Phi(x) \ = \ \exp\left(\frac{-\sigma^2x^2}{2}\right)\prod_{l=1}^{L'(s)}J_0\left(x\mid\gamma_{\mathrm{ch},l}\mid\right) \quad (8)$$

where ρ_n is the n-th root of the zeroth-order Bessel function $J_0(x)$, $J_1(x)$ is the first order Bessel function and σ^2 is the receiver noise power. The CDF of the received power is then equal to $\mathrm{F}(\mid\gamma_{\mathrm{T}}\mid)^2P_{\mathrm{t}}$.

Figs. 5 and 6 show the CDF of the received power for each of the 12 van positions for Tx1 and Tx2 respectively. The vertical solid line indicates the -70.5 dBm over-reach boundary whereas the leftmost slanted solid line illustrates the theoretical Rayleigh CDF. For clarity, only the CDF of the Rx points in the middle of the rail in each van position are shown. The figures show that over-reach occurs with high probability for both Tx cases especially when Rx is near Tx. To analyze which scatterers have high power contribution to the received power, the ratio of power contribution of each scatterer class to the received power, averaged at different horizontal distances from Tx are shown in Table 4.

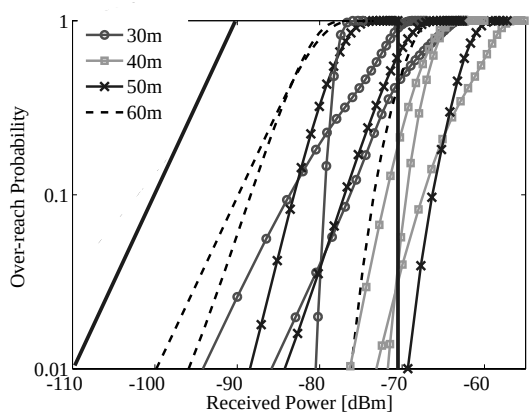

Figure 6 Received power CDF (over-reach probability) for Tx2. Solid line indicates the -70.5 threshold (straight) and theoretical Rayleigh CDF (slanted).

Table 4 Ratio of power contribution of scatterers to the mean received power for Tx1 and Tx2.

Distance from Tx1 [m]	LoS	ground	sidewalk	others
30	0.44	0.18	0.22	0.16
40	0.29	0.21	0.33	0.17
50	0.36	0.45	0.12	0.07
60	0.45	0.19	0.14	0.22
Distance from Tx2 [m]	LoS	ground	sidewalk	others
30	0.37	0.36	0.19	0.08
40	0.15	0.47	0.36	0.02
50	0.41	0.24	0.25	0.10
60	0.59	0.12	0.09	0.20

We observe that scatterers other than ground and sidewalk, denoted as 'others' in Table 4 comprise less than 22% of the received power. Hence the ground and sidewalk scatterers are generally dominant in any position. This hints the recommendation of employing absorbers to acquire a better performance for the DSRC system as is being done in ETC open road environment [24]-[25]. Figs. 7 and 8 show the CDF of the received power excluding the ground and sidewalk scatterings and it can be observed that the received power in most positions is now under the required threshold.

5. Over-reach prediction

In the previous section, we showed that the ground and sidewalk scatterers are the primary reason why over-reach occurs. It then suggests that the ground and sidewalk paths together with the LoS path may be used to predict over-reach.

Fig. 9 shows the median of the over-reach probability for Tx1 using all estimated paths (case 1) and using only

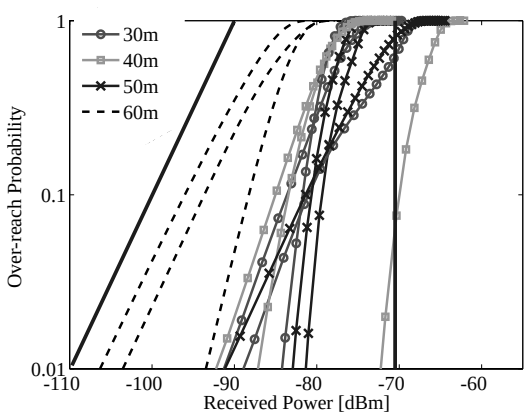

Figure 7 Received power CDF (over-reach probability) for Tx1 without ground and sidewalk scatterers. Solid line indicates the -70.5 threshold (straight) and theoretical Rayleigh CDF (slanted).

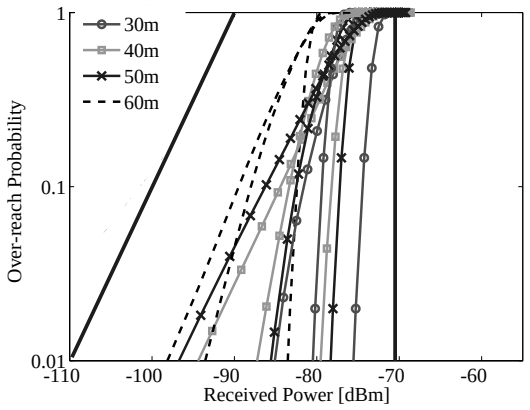

Figure 8 Received power CDF (over-reach probability) for Tx2 without ground and sidewalk scatterers. Solid line indicates the -70.5 threshold (straight) and theoretical Rayleigh CDF (slanted).

the LoS, ground and sidewalk paths (case 2). This figure shows the Rx points in the middle of the rail located 30 to 60 meters away from Tx1. For all positions, cases 1 (using all paths) and cases 2 (using only the LoS, ground and sidewalk paths) are very similar indicating that these paths can be used to predict over-reach. The same observations can be made for Tx2 as shown in Fig. 10.

6. Conclusion

The over-reach of radiated power from the DSRC service zone to the out-of-zone inside an arched transportation tunnel is analyzed. By conducting wideband directional channel soundings inside the tunnel, the parameters of the radio propagation paths such as angle-of-arrival, delay and complex path weights could be estimated by em-

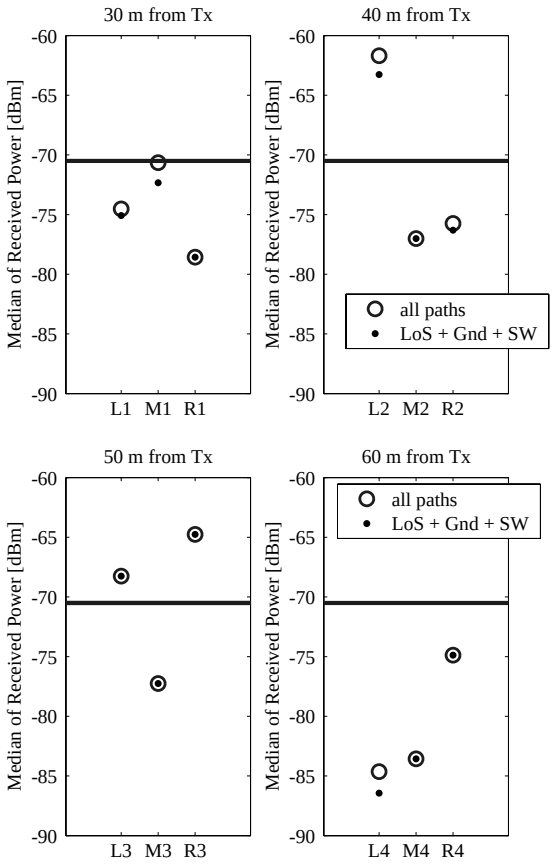

Figure 9 Median of over-reach probability for Tx1. (L, M and R corresponds to the left, middle and right lanes respectively as shown in Fig. 1).

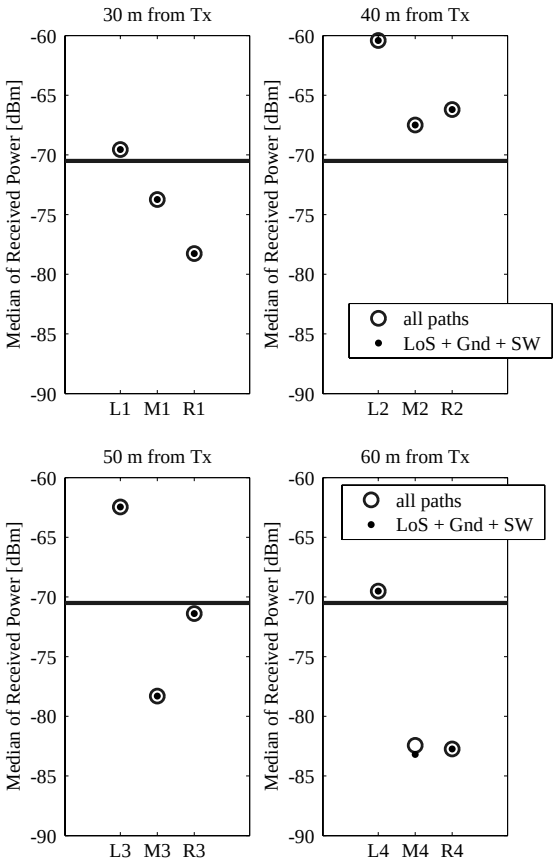

Figure 10 Median of over-reach probability for Tx2. (L, M and R corresponds to the left, middle and right lanes respectively as shown in Fig. 1).

ploying a multidimensional maximum likelihood parameter algorithm. The extracted paths are also classified according to the tunnel structure such as ground, sidewalk, walls, light-frame and ceiling. Using the path parameters together with application antennas that satisfy the threshold values of the DSRC standard, the delay spread and fluctuations of received power probability equivalent to the over-reach probability in the out-of-zone is predicted for 2 Tx antenna positions. The ratio of power contributions of the scatterers to the mean received power revealed that the dominant scatterers are due to the ground and sidewalk paths. This then suggests that the ground and sidewalk paths together with the LoS path can be used to predict the over-reach inside a typical transportation tunnel.

References

[1] D. Jiang, V. Taliwal, A. Meier, W. Holfelder, and R. Herrtwich, "Design of 5.9 ghz dsrc-based vehicular safety communication," *IEEE Wireless Communications,* vol. 13, pp. 36-43, Oct. 2006.

[2] A. Visser, H.H. Yakali,A.-J. van der Wees, M. Oud, G.A. van der Spek, and L.O. Hertzberger, "A hierarchical view on modeling the reliability of a DSRC link for ETC applications," *IEEE Trans. Intelligent Transportation Systems,* vol. 3, pp. 120-129, June 2002.

[3] J.P. Hubaux, S. Capkun, and J. Luo, "The security and privacy of smart vehicles," *IEEE Security & Privacy Magazine,* vol. 2, pp. 49-55, May 2004.

[4] ITS Handbook Japan 2002-2003. Available: http://www.its.go.jp/ITS/index/indexHBook.html

[5] Dedicated Short Range Communications. Available: http://grouper.ieee.org/groups/scc32/dsrc/

[6] A. G. Emslie, R. L. Lagace, and P. F. Strong, "Theory of the propagation of UHF radio waves in coal mine tunnels," *IEEE Trans. Antennas Propag.,* vol. AP-23, pp. 192-205, Mar. 1975.

[7] D. Didascalou, T. Schäfer, F. Weinmann, and W. Wiesbeck, "Ray-density normalization for ray-optical wave propagation modeling in arbitrarily shaped tunnels," *IEEE Trans. Antennas Propag.,* vol. 48, no. 9, pp. 1316-1325, Sep. 2000.

[8] K. Fujimori and H. Arai, "Propagation characteristics in tunnels including base station antenna," *Electron. and Commun. in Japan (Part I: Commun.),* vol. 84, iss. 4, pp. 1-10, April 2001.

[9] T. Imai, "Prediction of propagation characteristics in tunnels using ray-tracing method," *IEICE Trans. Commun. (Japanese Edition),* vol. J85-B, no. 2, pp. 216-226, Feb. 2002.

[10] K. Uchida, H. Nose, H. Maeda, and T. Matsunaga, "Theoretical and experimental study of propagation in 3D tunnels," *IEICE Trans. Commun.,* vol. E87-B, no. 10, pp. 3044-3049, Oct. 2004.

[11] Y. P. Zhang and H. J. Hong, "Ray-optical modelling of simulcast radio propagation channels in tunnels," *IEEE Trans. Veh. Technol.,* vol. 53, no. 6, pp. 1800-1808, Nov. 2004.

[12] M. Liénard, P. Degauque, J. Baudet, and D. Degardin, "Investigation on MIMO channels in subway tunnels," *IEEE J. Sel. Areas Commun.,* vol. 21, no. 3, pp. 332-339, April 2003.

[13] G. S. Ching, M. Ghoraishi, M. Landmann, N. Lertsirisopon, J. Takada, T. Imai, I. Sameda, and H. Sakamoto, "Wideband polarimetric directional propagation channel analysis inside an arched tunnel," submitted for 2nd review to *IEEE Trans. Antennas Propag.,*

[14] G. S. Ching, M. Ghoraishi, N. Lertsirisopon, J. Takada, I. Sameda, H. Sakamoto, and T. Imai, "Analysis of DSRC service over-reach inside an arched tunnel," *IEEE Journal on Selected Areas in Communication,* vol. 25, no. 8, pp. 1517-1525, Oct. 2007.

[15] G. S. Ching, M. Ghoraishi, N. Lertsirisopon, J. Takada, I. Sameda, R. Soma, H. Sakamoto, and T. Imai, "Analysis and modeling of DSRC service over-reach inside an arched transportation tunnel," in *Proc. 14th World Congress on Intelligent Transport Systems (ITS World Congress Beijing),* Beijing, China, Oct. 2007.

[16] "Dedicated Short-Range Communication System," ARIB STD-T75, Ver.1.0, Sep. 2001.

[17] "DSRC Application Sub-Layer," ARIB STD-T88, Ver.1.0, May 2004.

[18] T. Konda, "Shield tunneling method," *Civil Engineering, Japan Society of Civil Engineers,* vol. 39, pp. 23-27, July 2001.

[19] Rusk-Vector Channel Sounder. Available: http://www.channelsounder.de/

[20] R. S. Thomä, M. Landmann, G. Sommerkorn, and A. Richter, "Multidimensional high-resolution channel sounding in mobile radio," in *Proc. 21st IEEE Inst. Meas. Technol. Conf.,* 2004, pp. 257-262, May 2004.

[21] M. Steinbauer, A. Molisch, and E. Bonek, "The double-directional radio channel," *IEEE Antennas and Propagation Magazine,* vol. 43, No. 4, pp. 51-63, Aug. 2001.

[22] L. Correia, *Wireless Flexible Personalised Communications: COST 259: European Co-operation in Mobile Radio Research,* John Wiley and Sons, 2001.

[23] H. Zhu, J. Takada, K. Araki, and T. Kobayashi, "Verification of a two-dimensional/three dimensional hybrid ray-tracing method for spatiotemporal channel modeling," *Radio Science,* vol. 36, no. 1, pp. 53-66, Feb. 2001.

[24] R. K. Pokharel, M. Toyota, and O. Hashimoto, "Analysis on effectiveness of wave absorbers to improve DSRC electromagnetic environment on express highway," *IEEE Trans. Microw. Theory Tech.,* vol. 53, no. 9, pp. 2726-2731, Sep. 2005.

[25] K. Haneda, J. Takada, T. Iwata, Y. Wakinaka, and T. Kunishima, "Experimental determination of propagation paths for the ETC system–equipment development and field test– ," *IEICE Trans. Fundamentals,* vol. E87-A, no. 11, pp. 3008-3015, Nov. 2004.

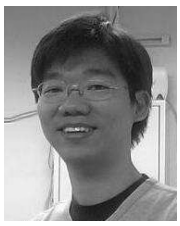

Gilbert Siy Ching was born in Manila, Philippines in 1974. He received his B.S. and M.S. degrees in electrical engineering from the University of the Philippines in 1996 and 2003, respectively and was also an instructor at the same university from 1996 to 2003. In 2007, he got his D.E. degree from Tokyo Institute of Technology, and is presently working in Kozo Keikaku Engineering, Inc. His current interests are in radio propagation channel measurements, analysis and modeling.

Dr. Ching was the recipient of the best student paper award from the area of Asia Pacific at the 17th International Symposium on Personal, Indoor and Mobile Radio Communications (PIMRC '06), and the First Prize for Best Student Scientific Paper from the 14th World Congress on Intelligent Transport Systems (ITS '07) . He is a member of the IEEE and the Institute of Electronics, Information and Communication Engineers (IEICE), Japan.

Mir Ghoraishi received M.E. from Amirkabir University of Technology (Tehran Polytechnic), Tehran, Iran, in electrical engineering in 1999.

He entered Tokyo Institute of Technology in 1999 to pursue his Ph.D. degree in wireless communication engineering. He is a researcher in Tokyo Institute of Technology since 2004. His research interests are wireless radio channel measurement and modeling, array antenna signal processing and calibration, and wireless positioning.

He is a member of IEEE and the Institute of Electronics, Information and Communication Engineers of Japan (IEICE).

Navarat Lertsirisopon was born in Bangkok, Thailand, in 1981. She received her B.E. degree from Sirindhorn International Institute of Technology, Thammasat University, Bangkok, Thailand in 2002 and received her M.E. degree from Tokyo Institute of Technology, Tokyo, Japan in 2006. Presently, she is studying towards the D.E. degree in Tokyo Institute of Technology, Tokyo, Japan. Her current research interest is propagation prediction modeling in wireless communication systems.

Ms. Lertsirisopon is a student member of the Institute of Electronics, Information and Communication Engineers (IEICE), Japan.

Jun-ichi Takada received the B.E., M.E., and D.E. degrees from the Tokyo Institute of Technology, Tokyo, Japan, in 1987, 1989, and 1992, respectively. From 1992 to 1994, he was a Research Associate Professor with Chiba University, Chiba, Japan. From 1994 to 2006, he was an Associate Professor with Tokyo Institute of Technology. Since 2006, he has been a Professor with Tokyo Institute of Technology. His current interests are wireless propagation and channel modeling, array signal processing, UWB radio, cognitive radio, and ICT for international development.

Dr. Takada is a member of IEICE,ACES, and the ECTI Association Thailand.

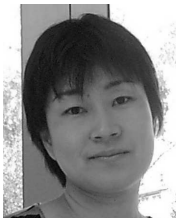

Itoji Sameda was born in Oita, Japan in 1968. She received her B.S and M.S degrees in electrical and electronics engineering from Nagasaki University, Japan in 1992 and 1994, respectively. She joined the Japan Highway Public Corporation in 1994. In 2005, the company was privatized and she is now with the ETC (Electronic Toll Collection) system section, Expressway Operation department, Kansai branch of West Nippon Expressway Co. Ltd. She is interested in wireless communication systems.

Ryuji Soma started working at the Japan Highway Public Corporation in 1978. He was then promoted to assistant chief of the Facilities Section at the Nippon Expressway Research Institute Co., Ltd. in 2004. Since 2008, he has worked as a manager of the Facilities Work Section, Hachioji Construction Office, Yokohama Branch of the Central Nippon Expressway Co., Ltd. ("NEXCO-Central"). He is engaged in the construction of the Tokyo Beltway infrastructure.

Hironori Sakamoto is with the Highway Telecom Engineering Co. Ltd., Japan.

Tetsuro Imai was born in Tochigi, Japan, in 1967. He received his B.S. and Ph.D. Degrees from Tohoku University, Japan, in 1991 and 2002, respectively.
He joined the Wireless System Laboratories of Nippon Telegraph and Telephone Corporation (NTT), Kanagawa, Japan, in 1991. Since then, he has been engaged in the research and development of radio propagation and system design for mobile communications. He is now Manager of the Radio Access Network Development Department, NTT DoCoMo, Inc., Kanagawa, Japan.
Dr. Imai is a Member of the Institute of Electronics, Information and Communication Engineers of Japan (IEICE).

Received date: 13 December 2007
Received in revised form: 2 June 2008
Accepted date: 13 June 2008
Editor: Kiyoshi Mizui